3D Radiative hydrodynamical simulations of stellar surfaces

Lionel Bigot
Observatoire de la Côte d'Azur

■ Objectives :

The role of convection in stellar physics

-Transports energy to the surface
-Mixes elements
-Drives magnetic dynamos
-Excites p-modes
-Modifies spectral lines

The need of 3D hydrodynamical simulations

-Convection is *by nature* a 3D, time-dependent,
and non-local process → Cannot be well described by 1D hydrostatic

-Determine stellar chemical abundances and Vrad from spectra
without free parameters.

■ Numerical approach :

Details of simulations

- 3D compressional hydrodynamics
- Radiative energy transfer (crucial!)
- Sufficient grid resolutions (~23 kms at 250^3)
- State-of-the-art equation-of-state and opacities (continuum and lines)

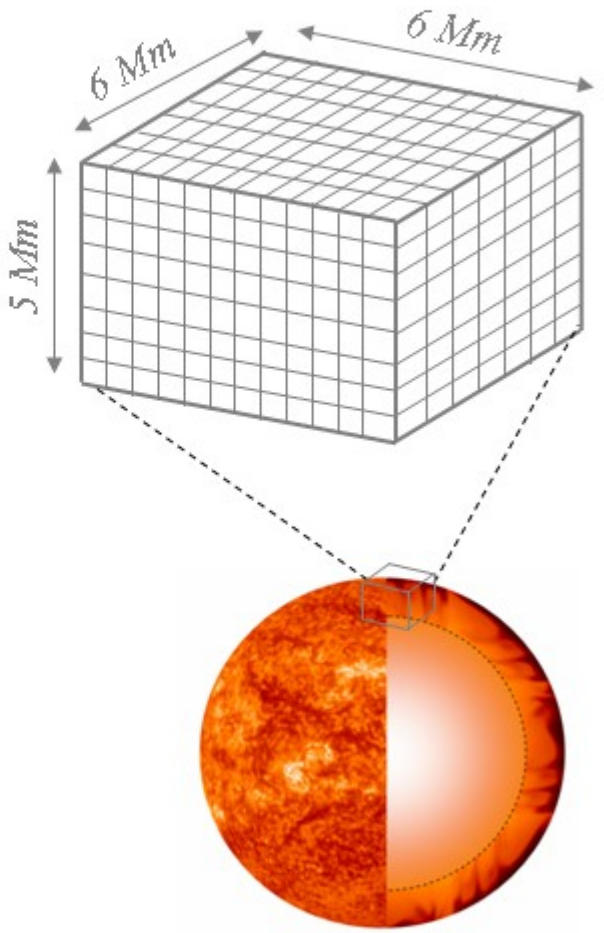

Parameters:

Effective temperature	: Teff
surface gravity	: log g
chemical composition	: [M/H]

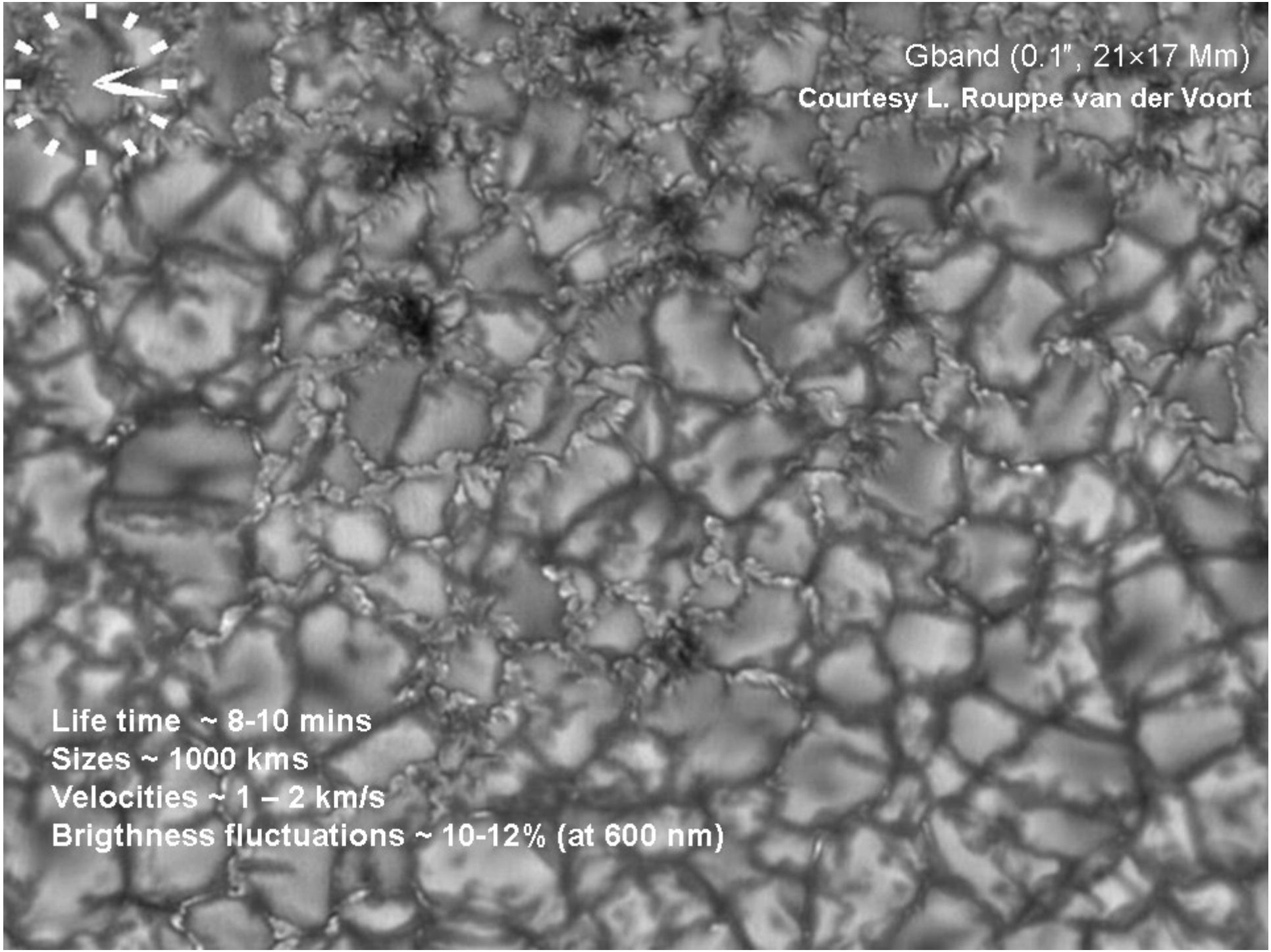
Gband (0.1", 21×17 Mm)
Courtesy L. Rouppe van der Voort
Life time ~ 8-10 mins
Sizes ~ 1000 kms
Velocities ~ 1 – 2 km/s
Brigthness fluctuations ~ 10-12% (at 600 nm)

Numerical approach :

Conservation of mass:

$$\frac{\partial \ln\rho}{\partial t} = -\bar{\mathbf{v}} \cdot \nabla \ln\rho - \nabla \cdot \bar{\mathbf{v}}$$

Conservation of momentum:

$$\frac{\partial \bar{\mathbf{v}}}{\partial t} = -\bar{\mathbf{v}} \cdot \nabla \bar{\mathbf{v}} + \bar{\mathbf{g}} - \frac{P}{\rho} \nabla \ln P + \nabla \cdot \sigma$$

Conservation of energy:

$$\frac{\partial e}{\partial t} = -\bar{\mathbf{v}} \cdot \nabla e - \frac{P}{\rho} \nabla \cdot \bar{\mathbf{v}} + Q_{\rm rad} + Q_{\rm visc}$$

$Q_{\rm rad}$ = radiative heating/cooling rate

Stein & Nordlund (1998)

■ Numerical approach :

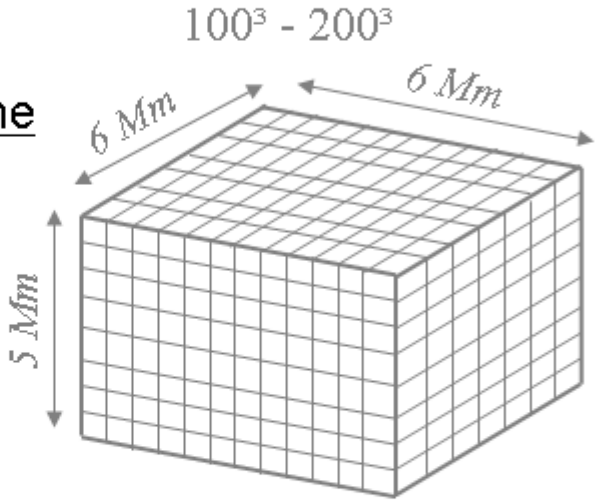

Spatial derivatives : High order (6th) compact scheme

$$\tfrac{1}{3}f'_{i-1} + f'_i + \tfrac{1}{3}f'_{i+1} = (f_{i-2} - 28f_{i-1} + 28f_{i+1} - f_{i+2})/(36\delta x),$$

$$\tfrac{2}{11}f''_{i-1} + f''_i + \tfrac{2}{11}f''_{i+1} = (3f_{i-2} + 48f_{i-1} - 102f_i + 48f_{i+1} + 3f_{i+2})/(44\delta x^2)$$

→ reach almost spectral accuracy
→ Stabilized by hyperviscosity viscosity

Time advance : 3rd order leap-frog

(predictor) $$f^{n+1/2} = af^{n-1} + (1-a)f^n + b\left(\frac{\partial f}{\partial t}\right)^n \Delta t$$

(corrector) $$f^{n+1} = af^{n-1} + (1-a)f^n + b\left(\frac{\partial f}{\partial t}\right)^n + c\left(\frac{\partial f}{\partial t}\right)^{n+1/2}$$

$a = r^3/(2+3r)$ $\quad c = (1+r)/(2+3r)$
$b = (1+r)^2/(2+3r)$ $\quad r = \Delta t^{n+1/2}/\Delta t^{n-1/2}$

■ Radiative transfer :

Stein & Nordlund (2002)

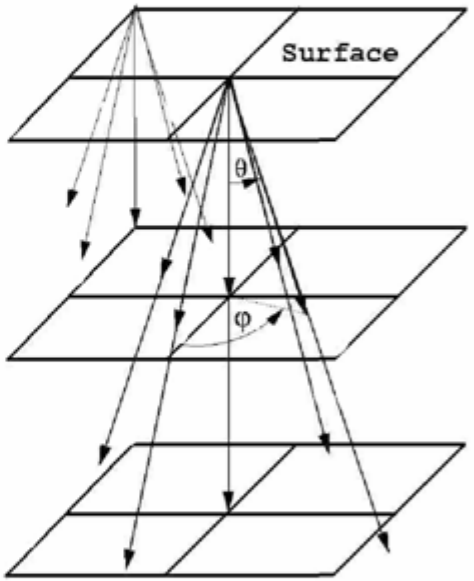

- Pure LTE (no scattering)
- Non-gray
- calculate cooling/heating J - B by solving Feautrier equations along 1 vertical + 4 inclined rays through each grid point at the surface

.

$$\mu = \cos\theta = 1, 1/3 \quad \left(w_\mu = 1/4, 3/4\right)$$

φ rotates by 15° at each time step

→ Interpolate source function + optical depth on the rays at each depth.

■ Radiative transfer :

$$Q_{rad} = 4\pi \int_{\lambda} \kappa_{\lambda}(J_{\lambda} - S_{\lambda}) d\lambda$$

Solve RT for q ≡ J - S to avoid roundoff errors at $\tau \rightarrow \infty$ (J→S)

$$q_{\lambda} = P_{\lambda} - S_{\lambda} \qquad P_{\lambda} = \frac{1}{2}\left(I_{\lambda}^{+} + I_{\lambda}^{-}\right)$$

Modified Feautrier scheme

$$\frac{d^2 q_{\lambda}}{d\tau_{\lambda}^2} = q_{\lambda} - \frac{d^2 S_{\lambda}}{d\tau_{\lambda}^2}$$

$$\frac{dq_{\lambda}}{d\tau_{\lambda}} = q_{\lambda} + S_{\lambda} - \frac{d\ S_{\lambda}}{d\tau_{\lambda}} \quad (\tau \rightarrow 0)$$

$$q_{\lambda} \rightarrow 0 \quad (\tau \rightarrow \infty)$$

■ Radiative transfer :

$$q^{\lambda}_{j-1}\left(\frac{1}{\tau^{\lambda}_{j}-\tau^{\lambda}_{j-1}}\frac{2}{\tau^{\lambda}_{j+1}-\tau^{\lambda}_{j-1}}\right)$$

$$-q^{\lambda}_{j}\left[1+\left(\frac{1}{\tau^{\lambda}_{j}-\tau^{\lambda}_{j-1}}+\frac{1}{\tau^{\lambda}_{j+1}-\tau^{\lambda}_{j}}\right)\frac{2}{\tau^{\lambda}_{j+1}-\tau^{\lambda}_{j-1}}\right]$$

$$+q^{\lambda}_{j+1}\left(\frac{1}{\tau^{\lambda}_{j+1}-\tau^{\lambda}_{j}}\frac{2}{\tau^{\lambda}_{j+1}-\tau^{\lambda}_{j-1}}\right)=S^{\lambda}_{j-1}\left(\frac{1}{\tau^{\lambda}_{j}-\tau^{\lambda}_{j-1}}\frac{2}{\tau^{\lambda}_{j+1}-\tau^{\lambda}_{j-1}}\right)$$

$$-S^{\lambda}_{j}\left[\left(\frac{1}{\tau^{\lambda}_{j}-\tau^{\lambda}_{j-1}}+\frac{1}{\tau^{\lambda}_{j+1}-\tau^{\lambda}_{j}}\right)\frac{2}{\tau^{\lambda}_{j+1}-\tau^{\lambda}_{j-1}}\right]+S^{\lambda}_{j+1}\left(\frac{1}{\tau^{\lambda}_{j+1}-\tau^{\lambda}_{j}}\frac{2}{\tau^{\lambda}_{j+1}-\tau^{\lambda}_{j-1}}\right)$$

Stein & Nordlund (2002)

$$A^{\lambda}_{j}q^{\lambda}_{j-1}+B^{\lambda}_{j}q^{\lambda}_{j}+C^{\lambda}_{j}q^{\lambda}_{j+1}=D^{\lambda}_{j}$$

→ Gauss elimination of a tridiagonal matrix (forward elimination, backward substitution)

Radiative transfer - opacity binning

3D RT more CPU demanding than 1D (Nx × Ny × Nφ × Nt ~ 10^(7-8) !)

→ Cannot solve RT for thousand of lines
→ **opacity binning method** (Nordlund 1982, Sharklien 2000)

The wavelengths that reach $\tau\lambda \approx 1$ at the same depth are collected in one bin

$$Q_{rad} = \int_{\lambda} \kappa_{\lambda}(J_{\lambda} - S_{\lambda})d\lambda = \sum_{i} \sum_{j(i)} \kappa_{\lambda_j}(J_{\lambda_j} - S_{\lambda_j})w_{\lambda_j}$$

Wavelength index within bin i

Group index
i=0 (continuum), 2 - 3 (weak, intermediate and strong lines)
Assume K ~ 10^i * K_0

■ Radiative transfer - continuum and line opacities

Continuum opacities (Uppsala, Gustafsson et al. 1975 + updates)

$$\kappa = x_\kappa \kappa_{\rm cR}$$

$$x_\kappa = e^{-30\tau_{\rm cR}} \frac{\langle\kappa\rangle_J}{\langle\kappa\rangle_{\rm cR}} + \left(1 - e^{-30\tau_{\rm cR}}\right) \frac{\langle\kappa\rangle_{\rm (L+c)R}}{\langle\kappa\rangle_{\rm cR}}$$

$$\langle\kappa\rangle_J = \frac{\sum_j \kappa_{\lambda_j} J_{\lambda_j} e^{-\tau_{\lambda_j}/2} w_{\lambda_j}}{\sum_j J_{\lambda_j} e^{-\tau_{\lambda_j}/2} w_{\lambda_j}} \qquad \frac{1}{\langle\kappa\rangle_{\rm cR}} = \frac{\sum_{j(i=1)} \frac{1}{\kappa_{\lambda_j}+\sigma_{\lambda_j}} \frac{\partial B_{\lambda_j}}{\partial T} w_{\lambda_j}}{\sum_{j(i=1)} \frac{\partial B_{\lambda_j}}{\partial T} w_{\lambda_j}}$$

Line ODF
(Castelli & Kurucz 2004)

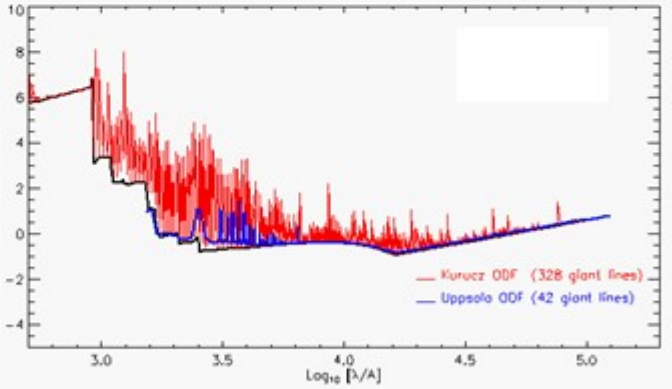

→ **Store in table K(ρ,T)** (for details, see Stein & Nordlund 2002)

■ **Radiative transfer :**

$$Q_{rad} = 4\pi\rho \sum_{\Omega} \sum_{i} \kappa_i q_i w_i w_\Omega$$

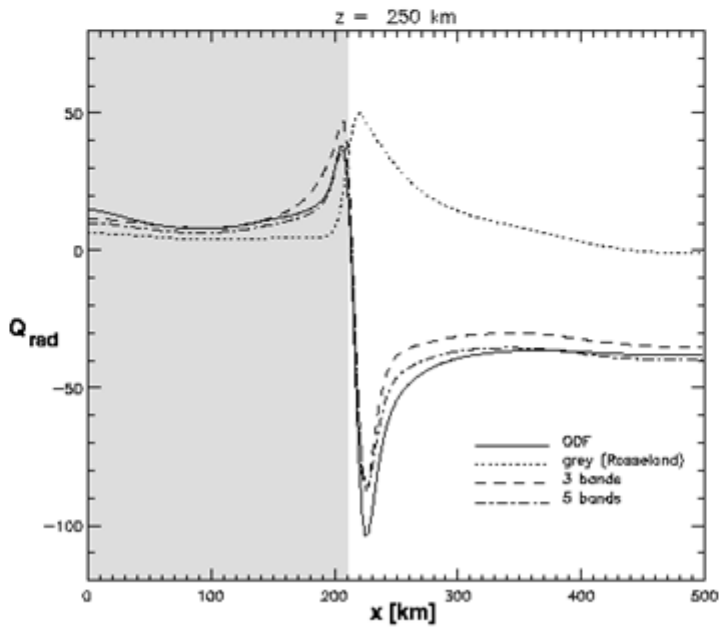

Courtesy A. Vögler, M. Schüssler

Convection properties - 3D structure

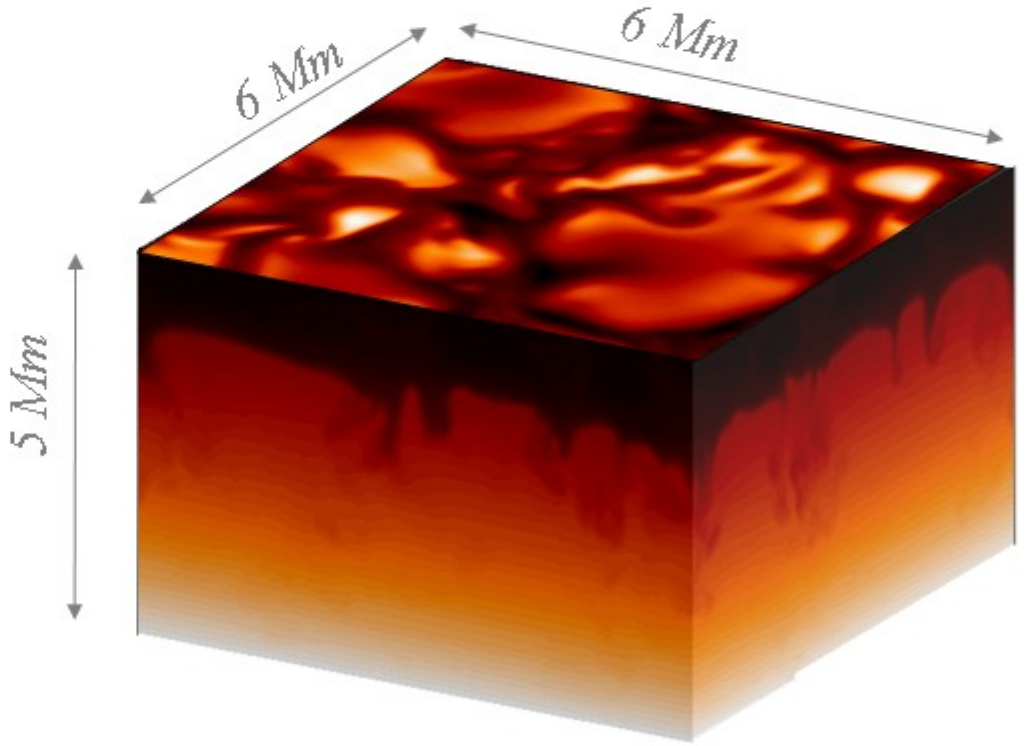

- 253 × 253× 163
- 9 rays /LTE
  (2 μ, 4φ + 1 vert.)
- 4 bins
- 1 snap / min

Bigot (2006)

Convection properties - surface intensity

Raw ($253^2 \times 163$)

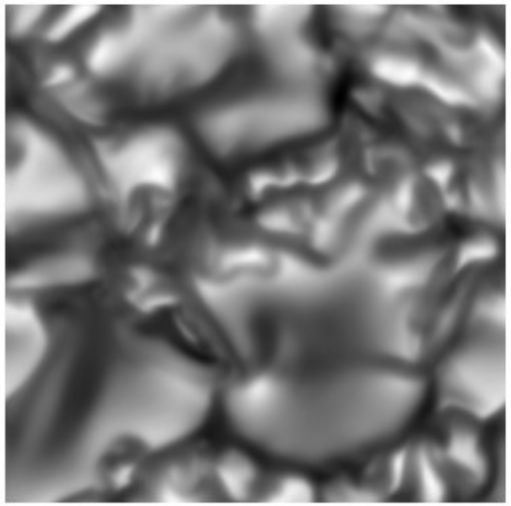

Raw ($253^2 \times 163$) + psf+noise

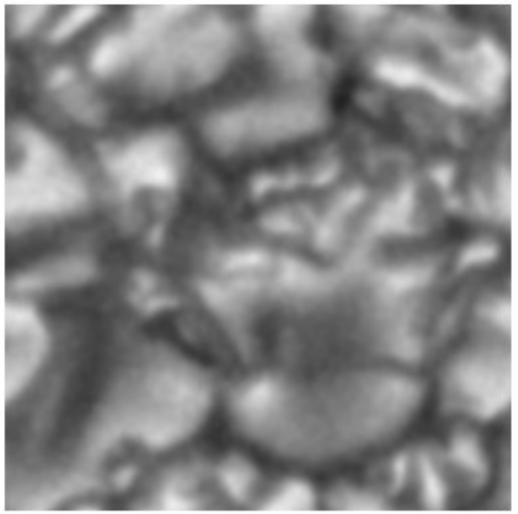

Solar Swedish Telescope 2004

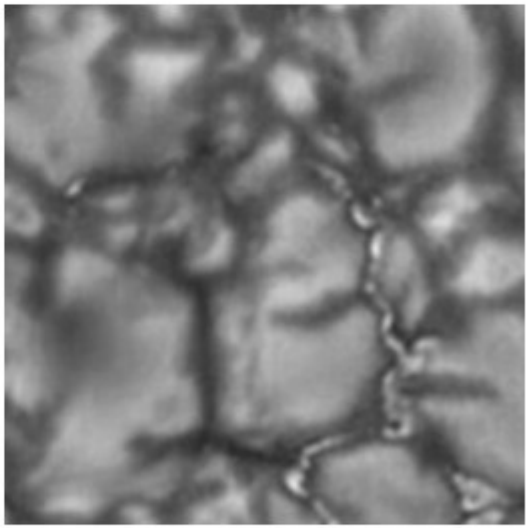

Courtesy L. Rouppe van der Voort

Convection properties - Velocity field

Intergranular lane

Granules
"Fountain-like" behaviour

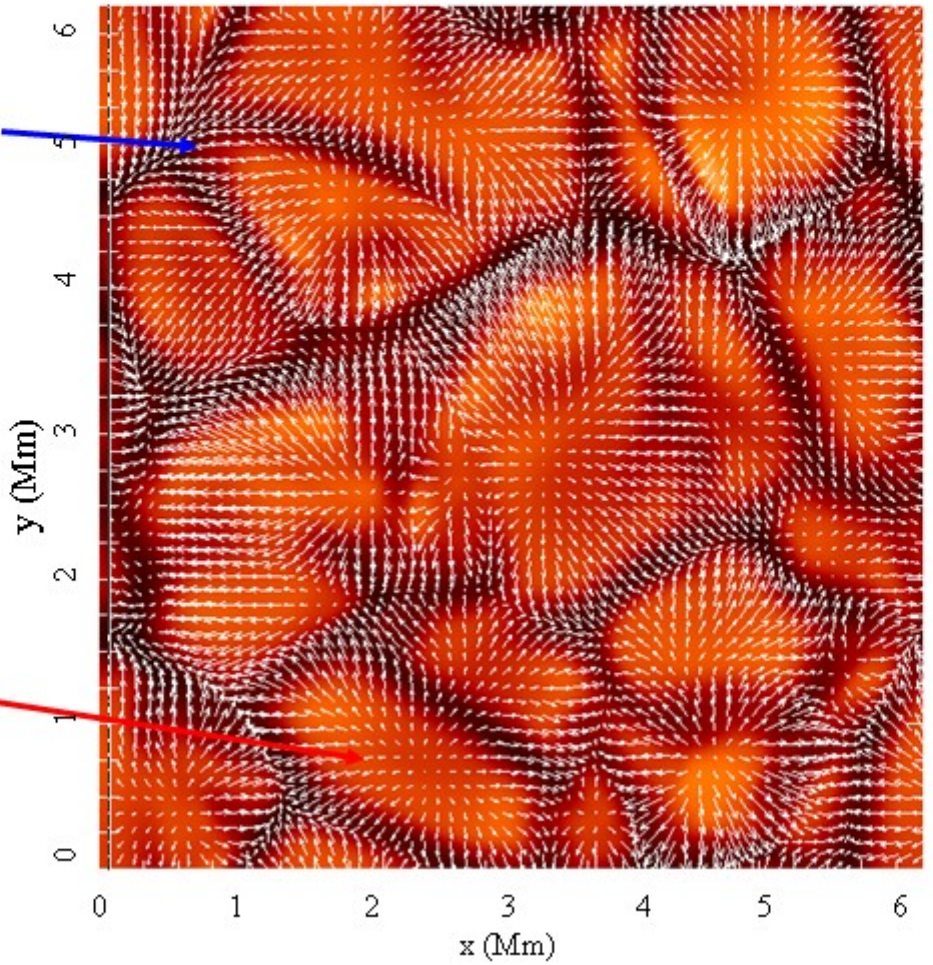

Convection properties - Velocity field

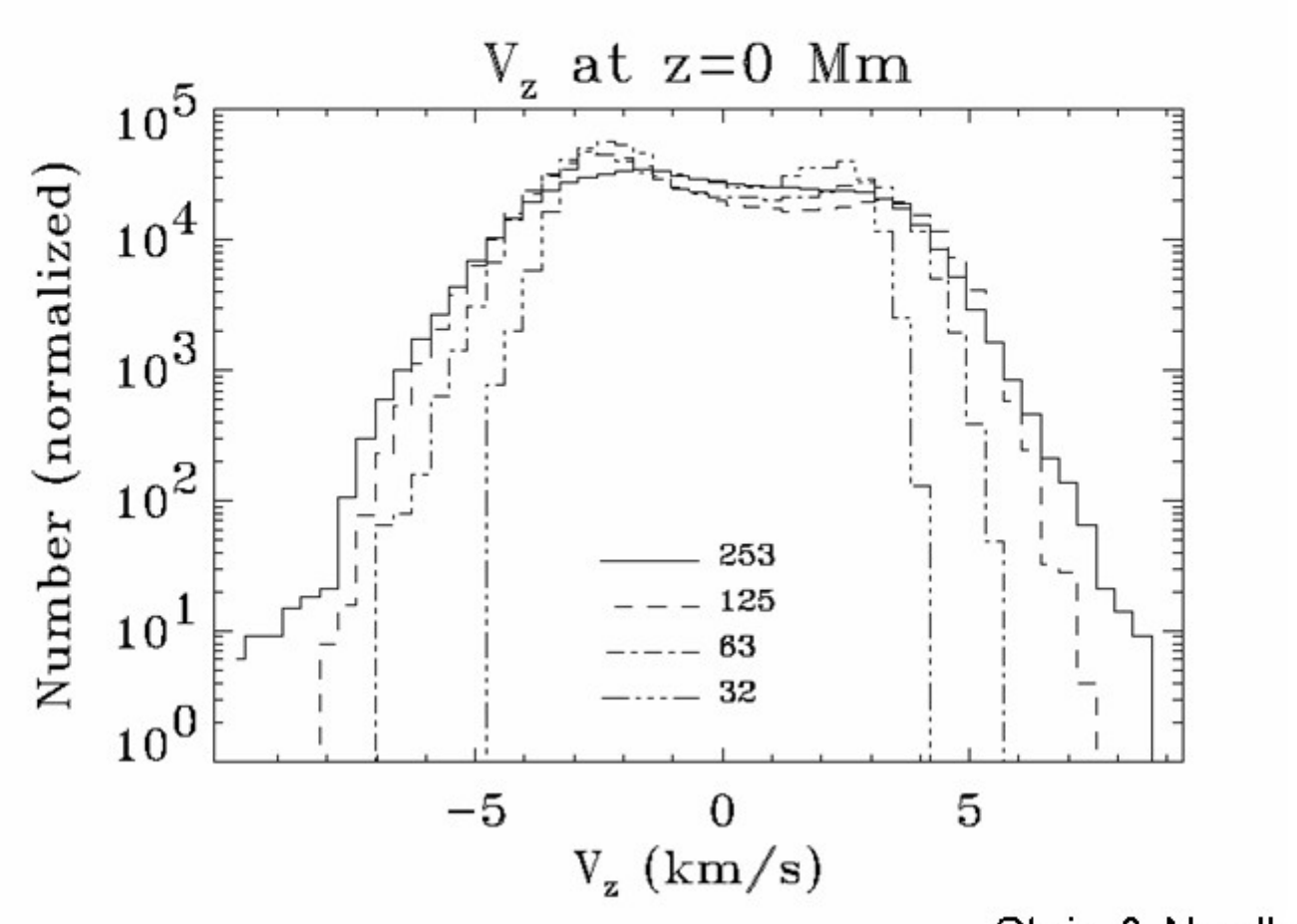

Stein & Nordlund (1998)

Convection properties - vorticity

Granules
≈ laminars

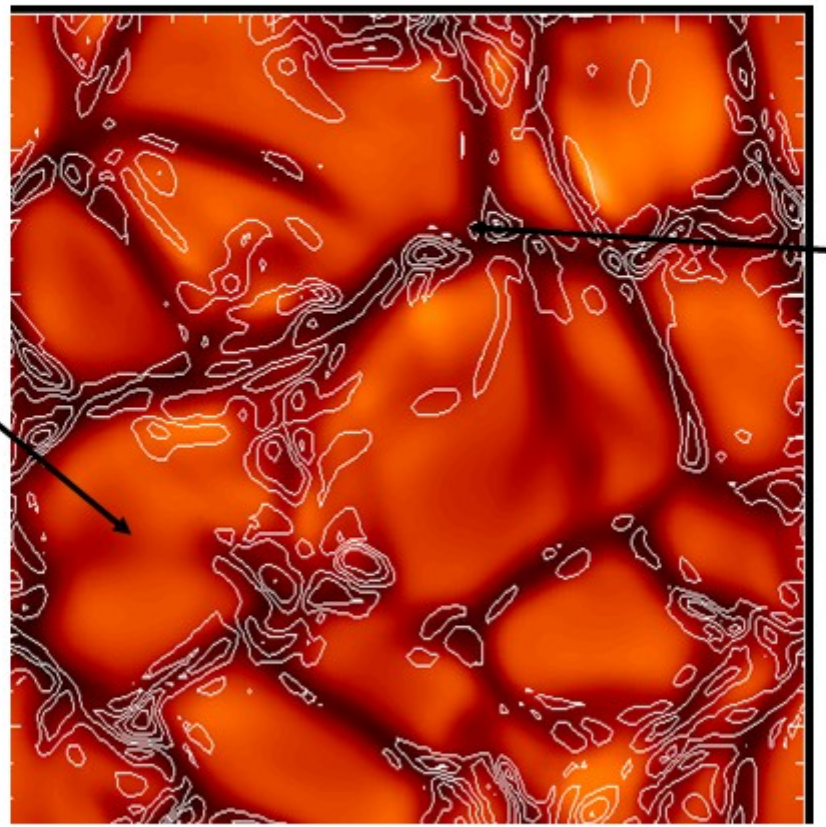

Inter-granular
= turbulent

- **Convection properties - vorticity**

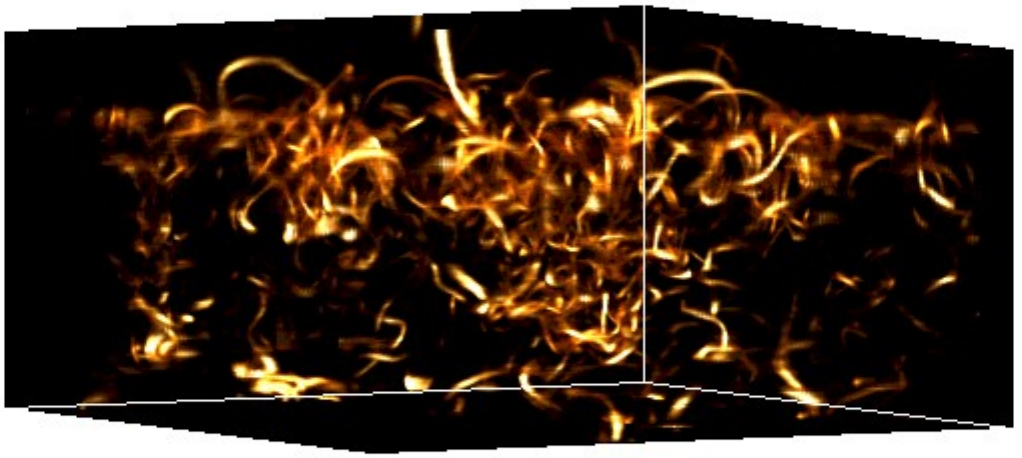

Courtesy B. Stein & A. Nordlund

Convection properties - structure

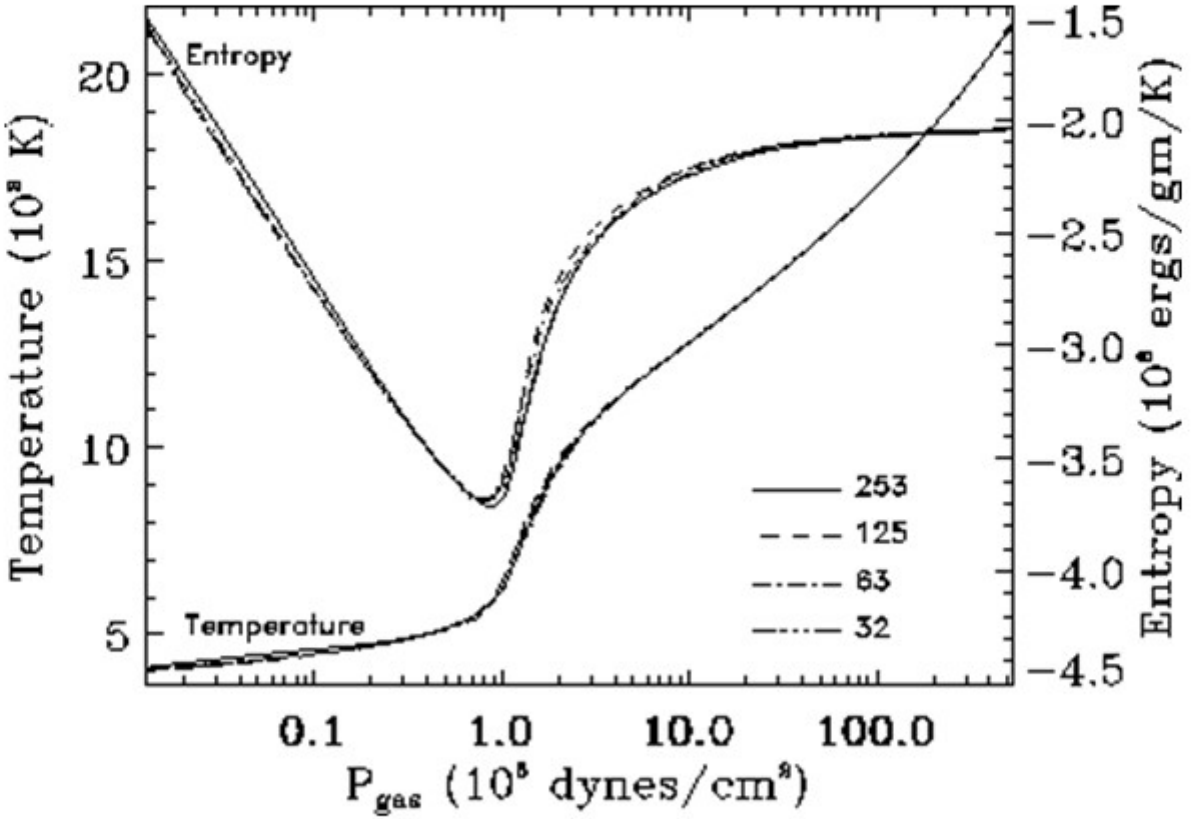

Nordlund (Granada workshop 1998)

Convection properties - structure

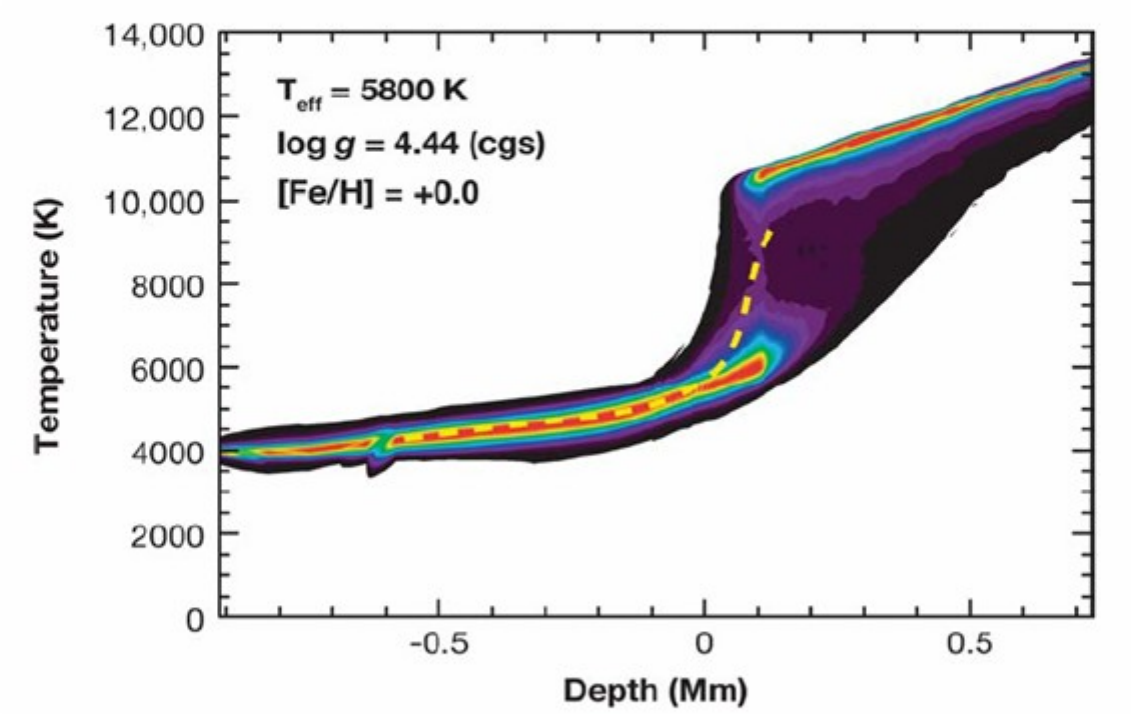

Asplund (2005)

→ Small corrections for solar type stars at [Fe/H] ~ $[Fe/H]_{\odot}$

Convection properties - brighness fluctuations

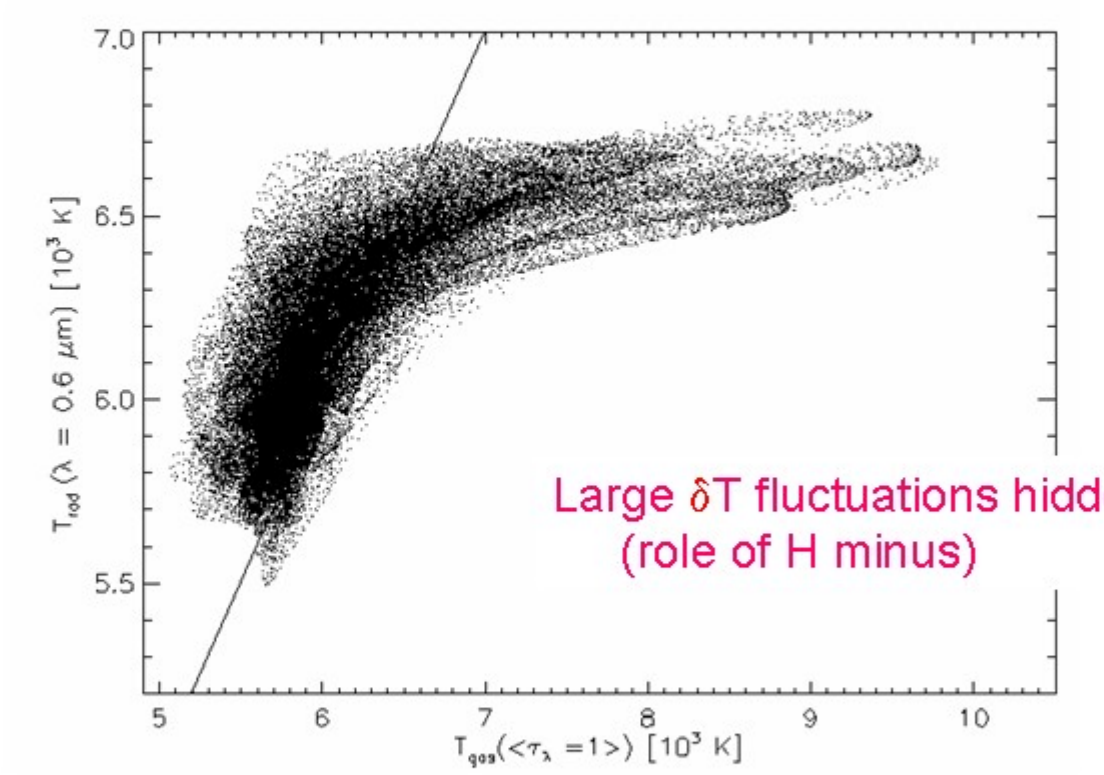

Large δT fluctuations hidden !
(role of H minus)

δT_{rad} rms = 4.2%

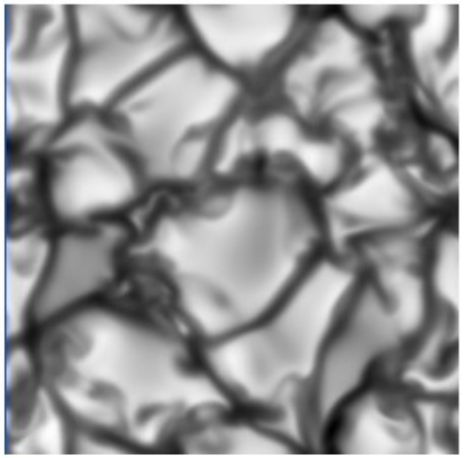

δT_{gas} rms = 11.9%
($<\tau_{0.6\mu m}>=1$)

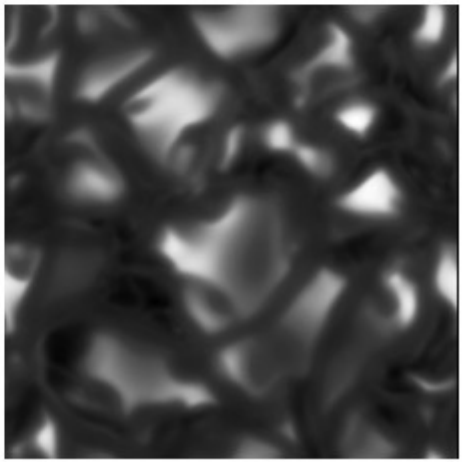

→ for given Teff, 3D temperature > 1D temperature !

λ = 0.6 μm : δI rms (simu+psf)= 12% (17% without psf)

Convection properties - brighness fluctuation

δI rms = 18%

δI rms = 15%

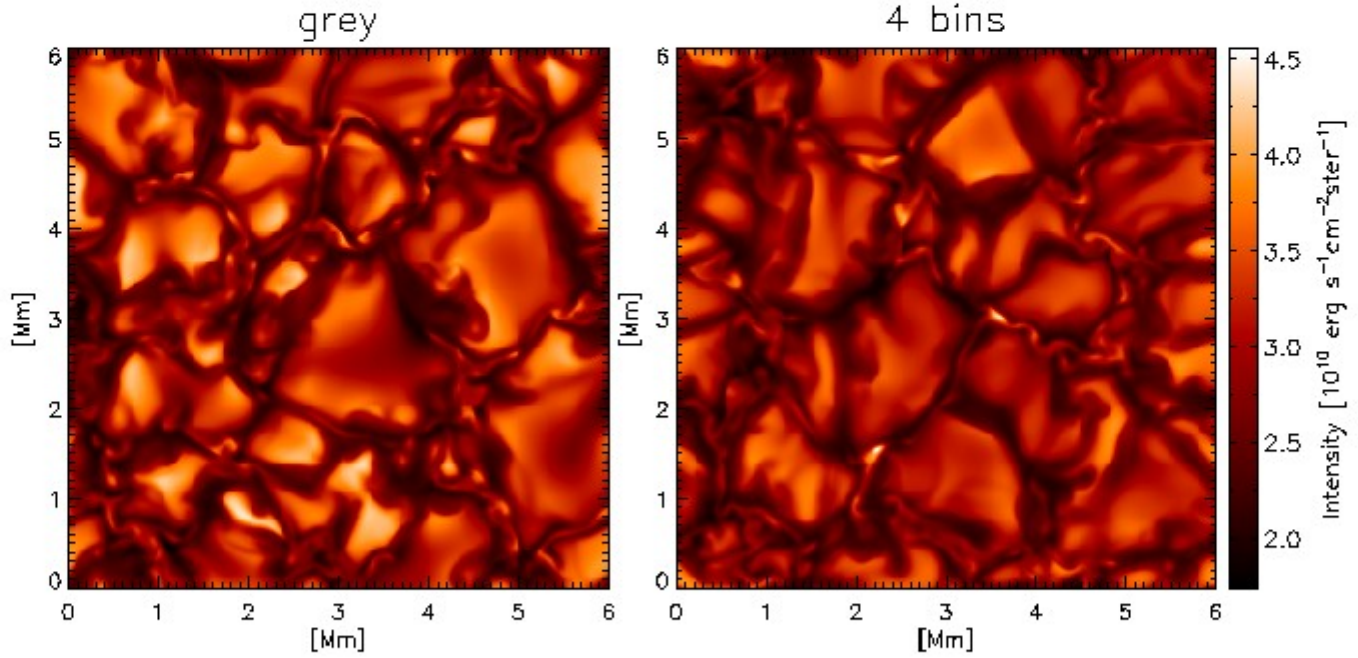

Vögler (2004)

Spectral line synthesis

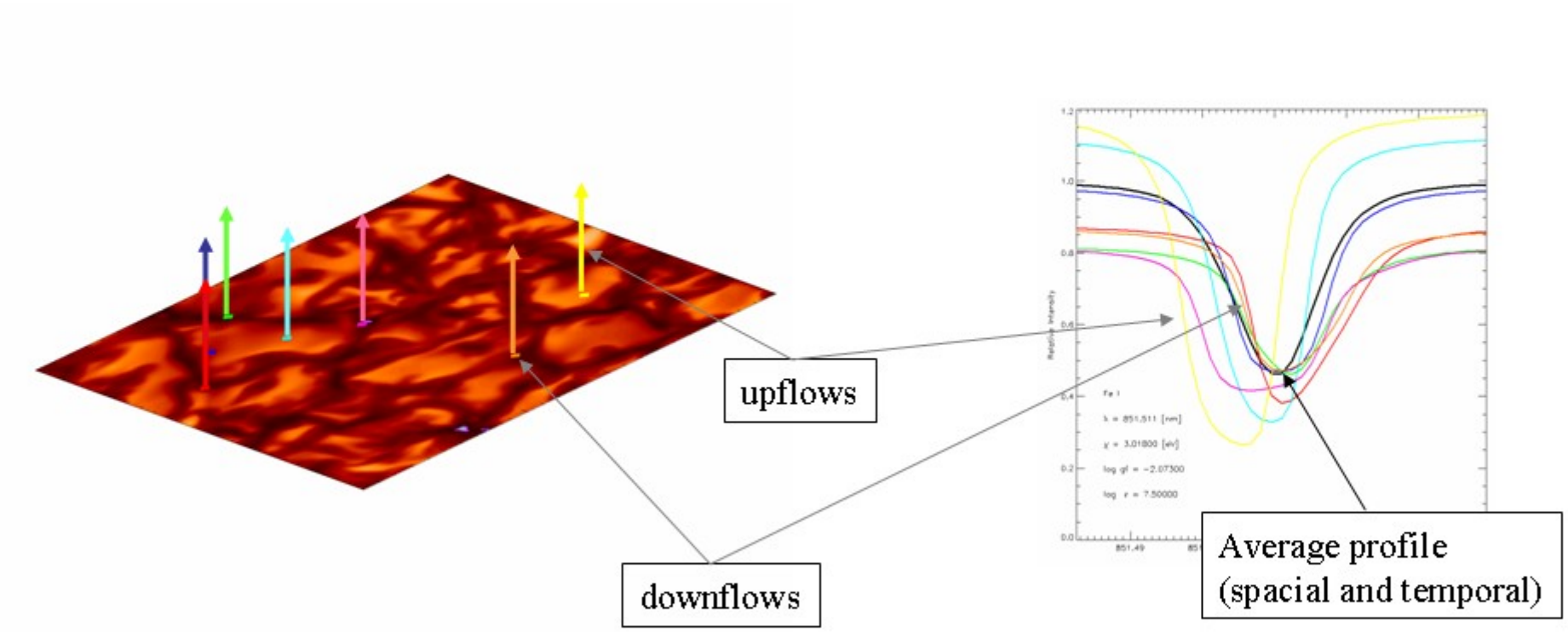

The final line profile is the result of a temporal and horizontal averages

Spectral line synthesis - effects of stratification

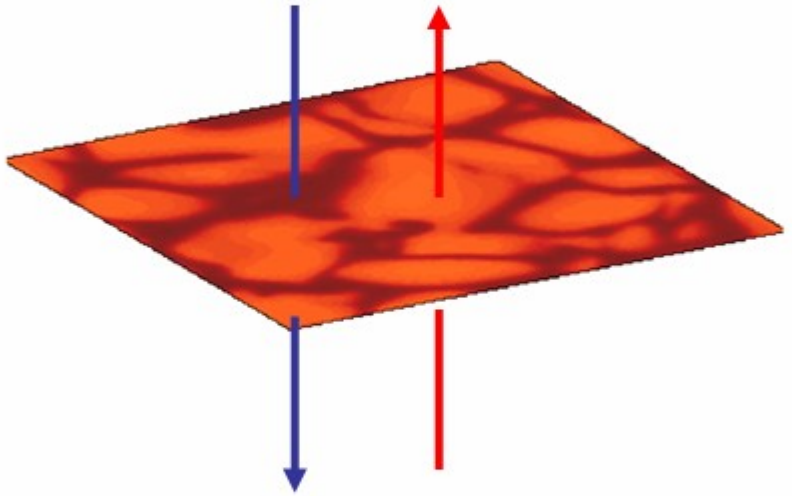

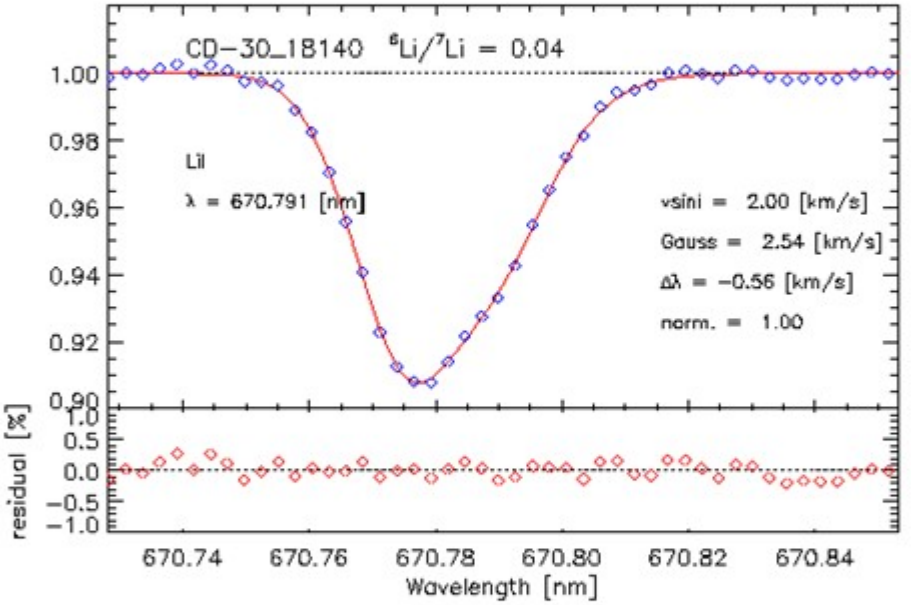

Nissen et al. (2000)

→ Asymetric line profiles reflect the asymetry between up- and downflows !

Spectral line synthesis - convective shifts

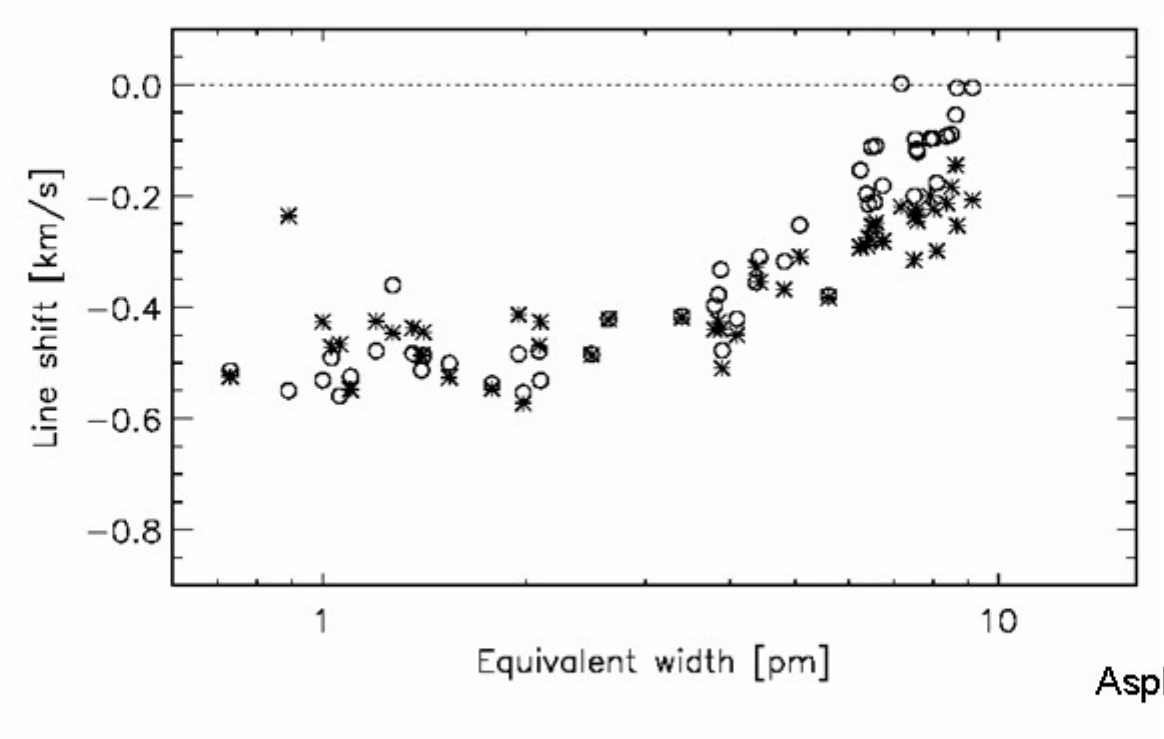

Asplund et al. (2000)

Important when measuring radial velocities (e.g. Gaia)

Spectral line synthesis - without velocity

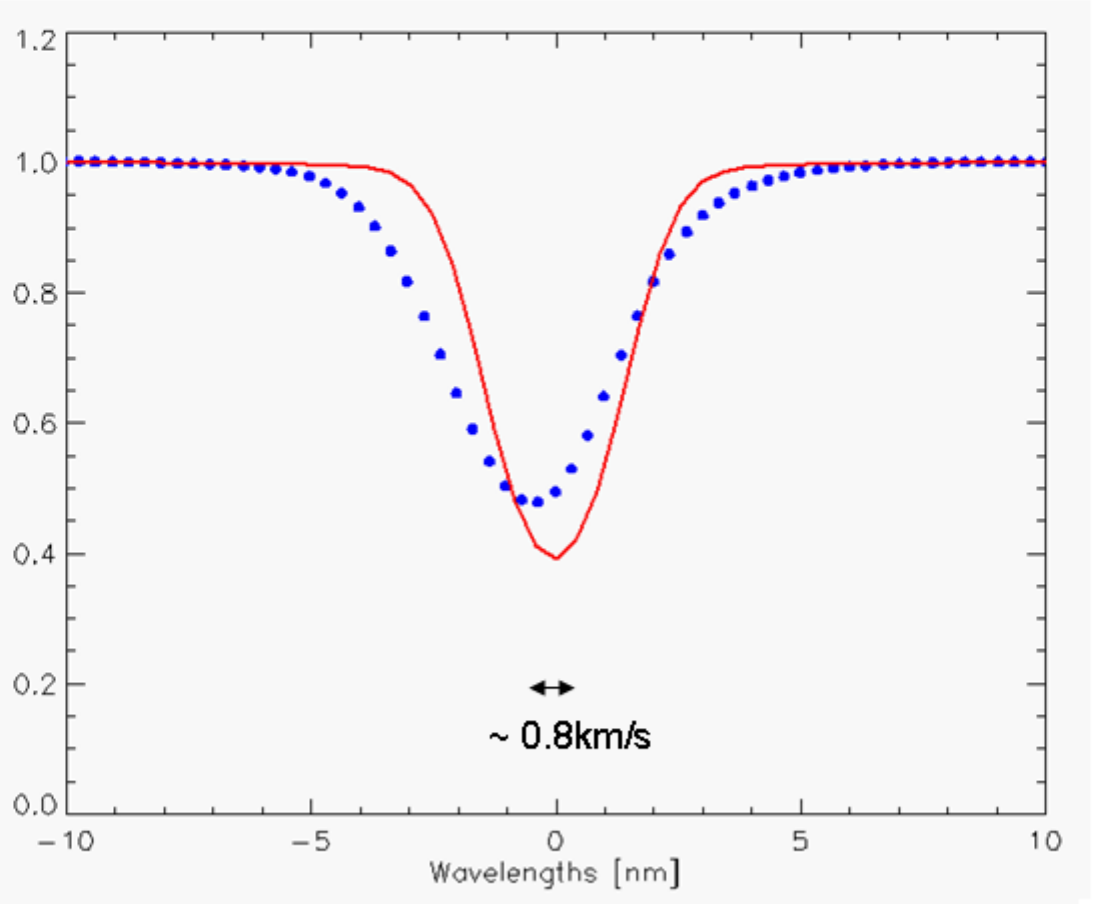

FeI 615.16 nm

Shape, shift, depth → all wrong !

Spectral line synthesis - with velocity

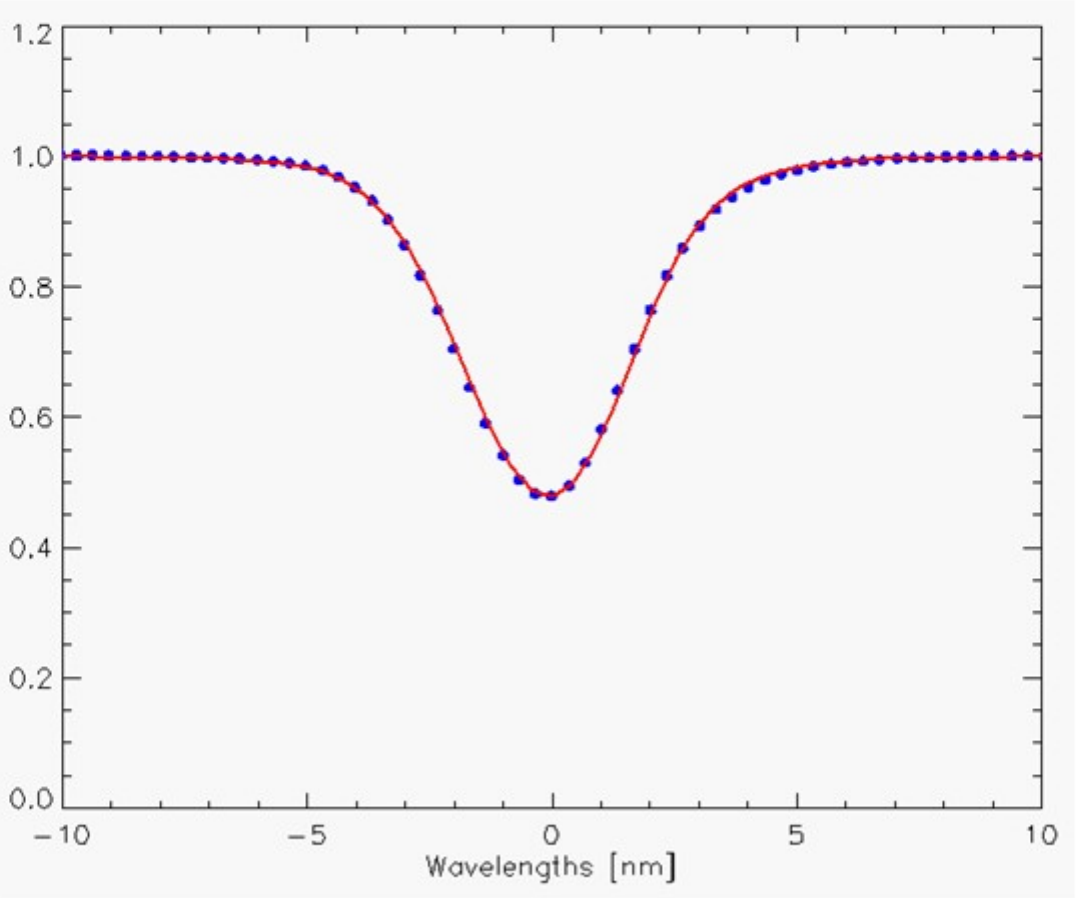

FeI 615.16 nm

No need of tuned parameters !

Spectral line synthesis - effects of numerical resolution

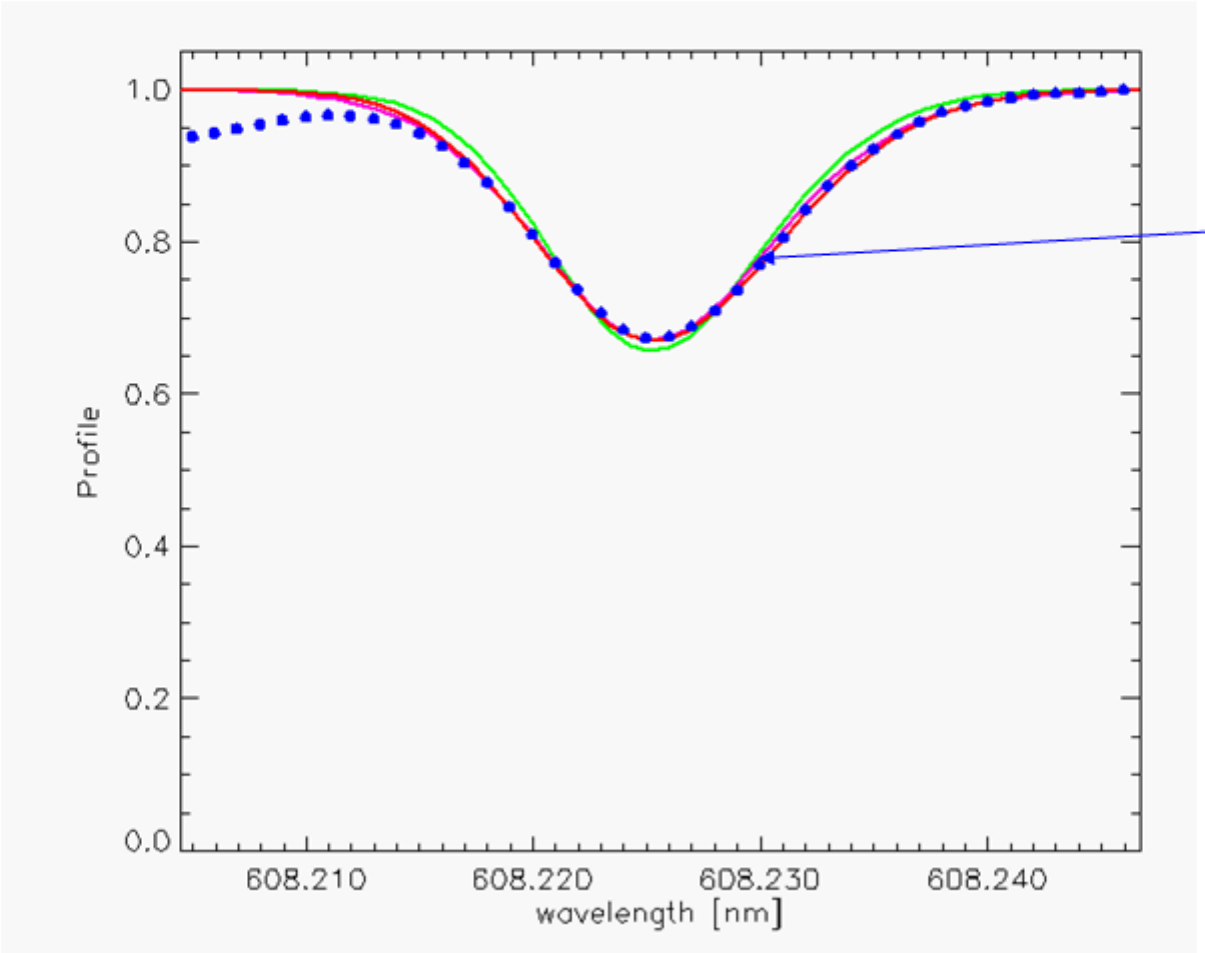

Observations
αCenA (Harps)

Fe I 608.27nm
log ε = 7.63

63 × 63 × 63

125 × 125 × 82

253 × 253 × 163

Spectral line synthesis - effects of numerical resolution

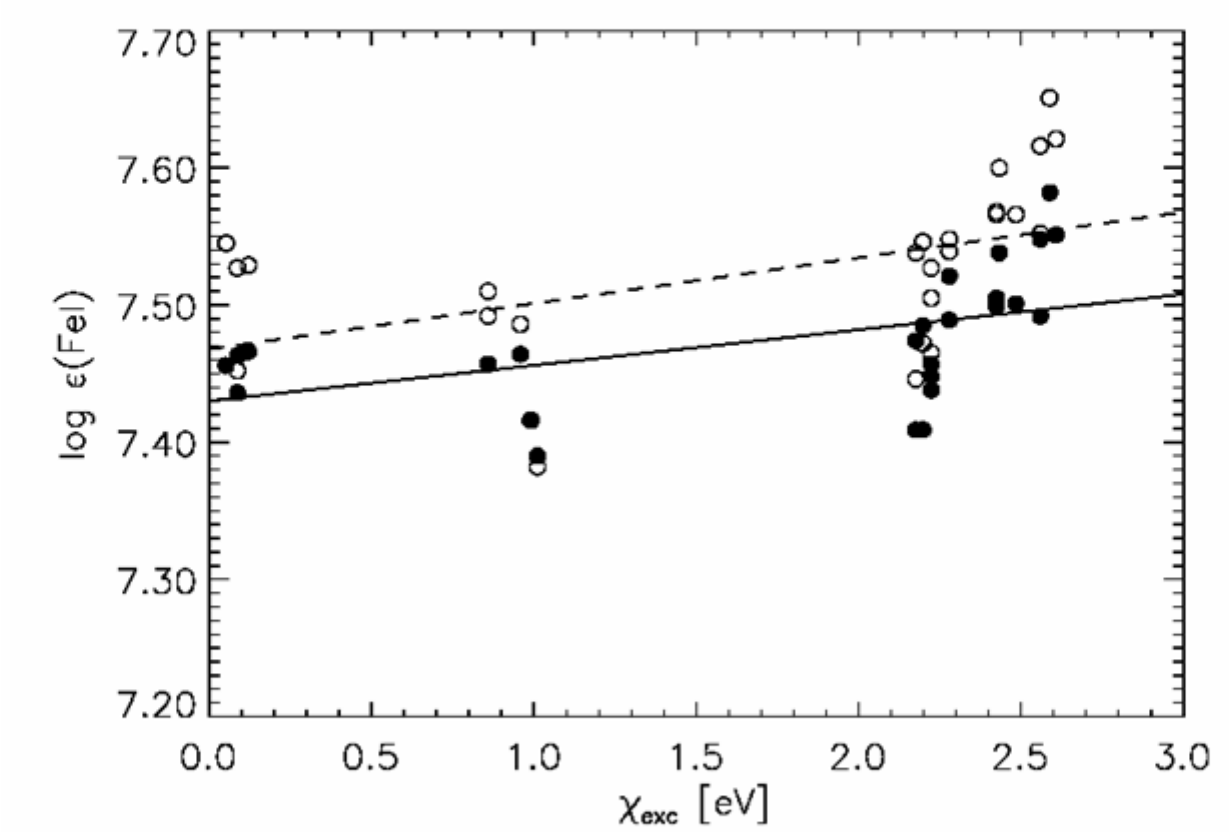

- ● $200 \times 200 \times 82 \rightarrow 7.48$
- ○ $50 \times 50 \times 63 \rightarrow 7.53$

Solar Fe abundance
Asplund et al. (2000)

Spectral line synthesis - Chemical abundances – 3D vs 1D

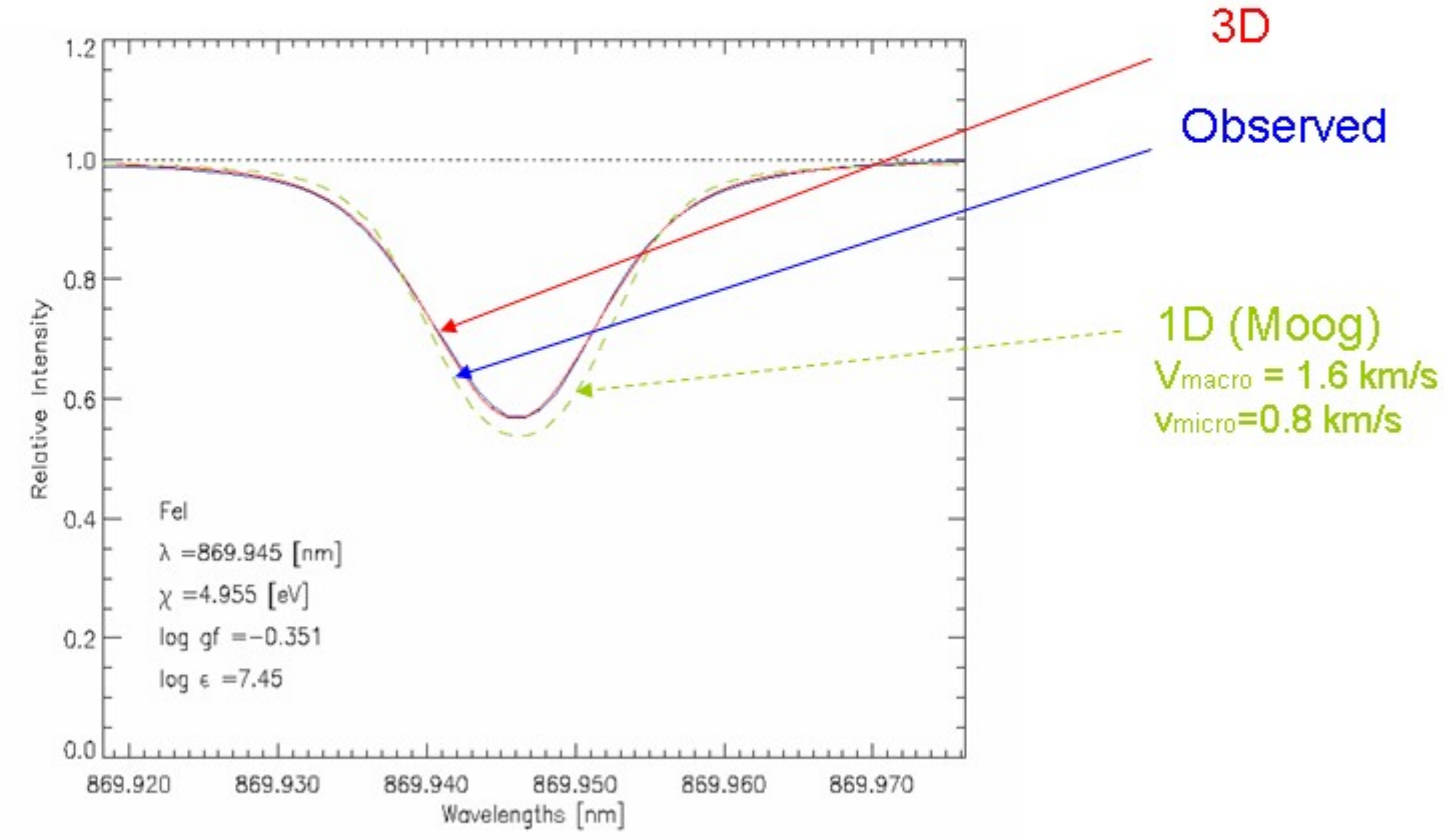

Bigot & Thévenin (2006)

Spectral line synthesis - Chemical abundances – 3D vs 1D

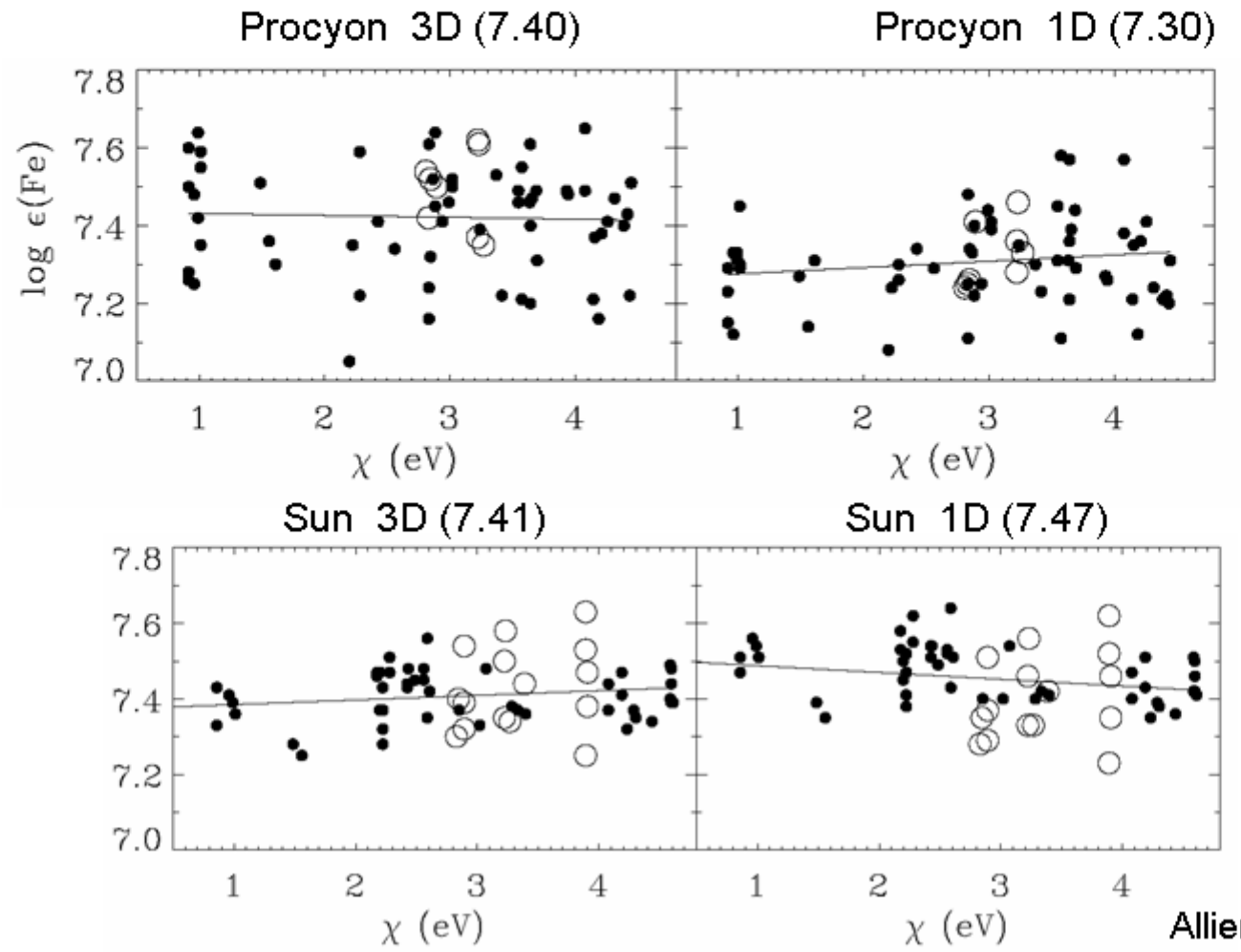

Δε (FeI) = +0.1 dex

Δε (FeI) = -0.06 dex

Alliende Prieto al. (2002)

Spectral line synthesis - Chemical abundances – oxygene problem

Asplund et al. (2004) re-derived [O]-abundance

→ New solar [O] = 8.66 (was 8.93)

→ **correction 0.27 dex** = (3D + NLTE)

lines	$\log \epsilon_O$		
	3D	*HM*	MARCS
[O I]	8.68 ± 0.01	8.76 ± 0.02	8.72 ± 0.01
O I	8.64 ± 0.02	8.64 ± 0.08	8.72 ± 0.03
OH vib-rot	8.61 ± 0.03	8.87 ± 0.03	8.74 ± 0.03
OH rot	8.65 ± 0.02	8.82 ± 0.01	8.83 ± 0.03

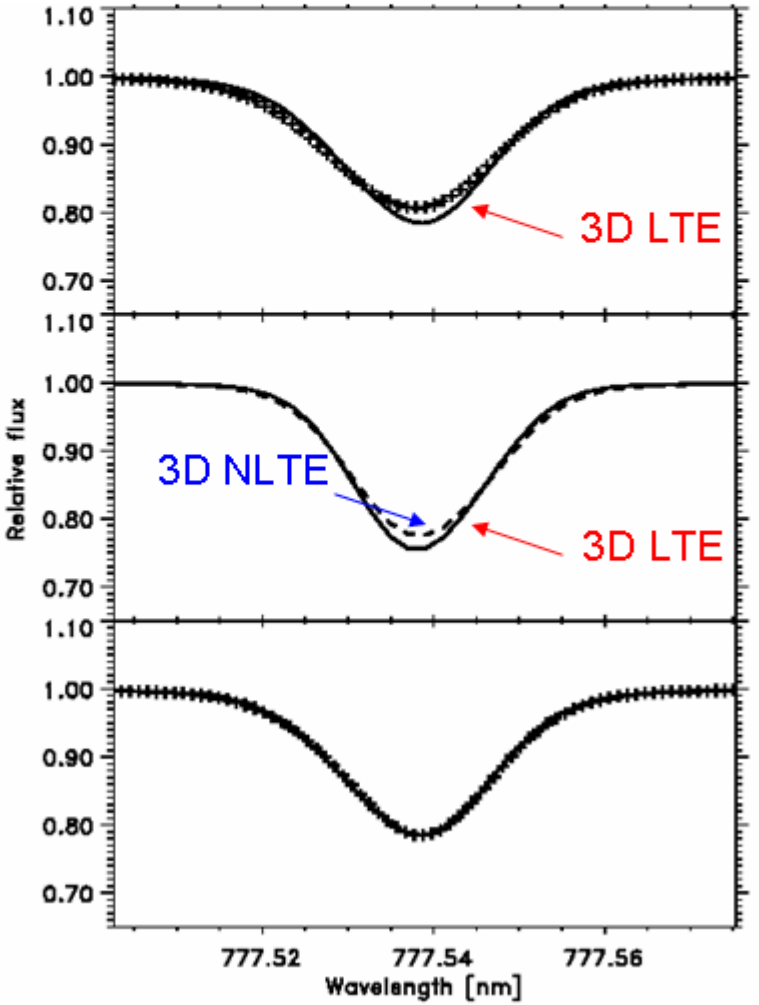

■ Spectral line synthesis - Chemical abundances – oxygene problem

Decrease of solar abundances O (48%), C (35%), N (27.5%), Fe (12%) … (Asplund et al. 2005)

→ **new metalicity Z = 0.012** (was 0.018, Grevesse & Sauval, 1998)

With new CNO (Asplund et al. 05)

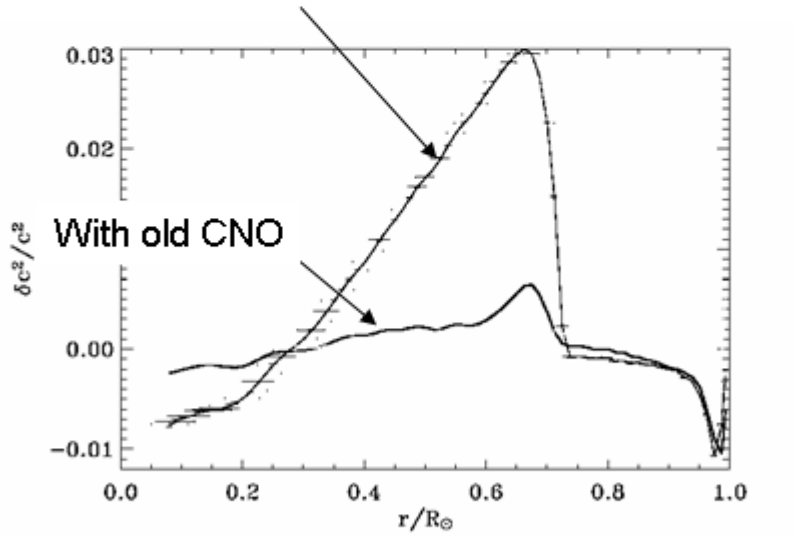

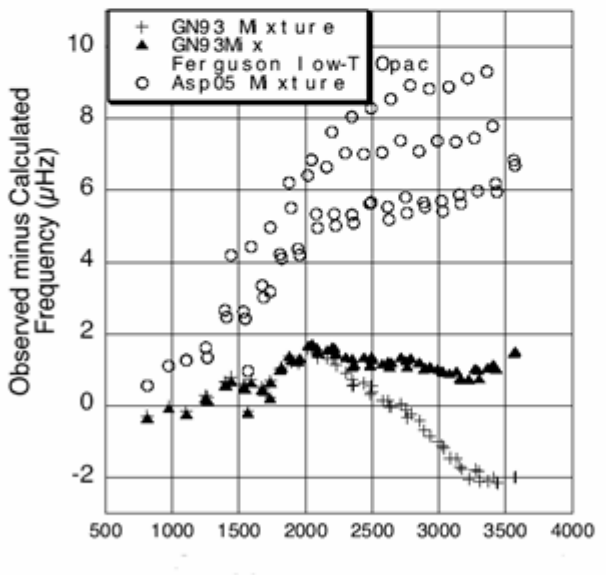

Guzik et al. (2006)

→ Disagreements with helioseismology !

→ change of [Ne/H], opacity increase etc but cannot restore agreement

■ Spectral line synthesis - Chemical abundances – metal poor stars

Asplund (2005)

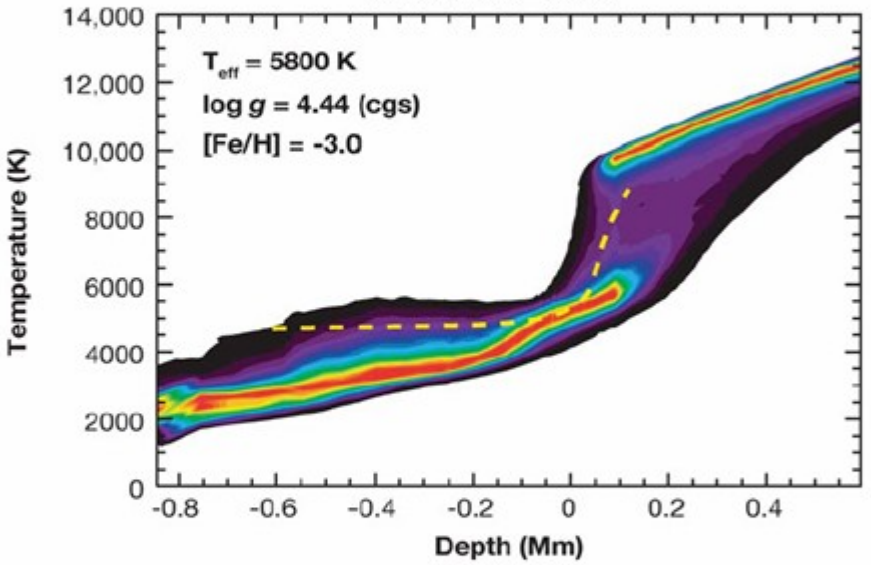

LTE analysis Asplund et al. 1999

Line	HD 140283		HD 84937	
[nm]	3D	1D[a]	3D	1D[a]
Li I 670.8	1.78	2.12	2.08	2.28
Be II 313.1	−0.92	−1.06	−0.85	−0.88
B I 249.8	−0.41	−0.21		
O I 777.2	7.20	7.15	7.32	7.30
K I 769.9	2.60	2.74		
Ca I 616.2	3.62	3.77	4.22	4.35
Fe I[b]	4.57 (0.16)	5.02 (0.17)	5.10 (0.12)	5.37 (0.11)
Fe II[b]	5.16 (0.10)	5.08 (0.11)	5.38 (0.02)	5.35 (0.03)
Ba II 614.2	−1.28	−1.12	−0.22	−0.05

Lack of spectral lines → convective cooling dominate

→ Much steeper gradients than 1D.
→ **Large** corrections for solar type stars at [Fe/H] << [Fe/H]⊙
→ Needs of 3D NLTE for definitive conclusion (e.g. Cayrel et al. 2007 for Li)

■ Spectral line synthesis - Red Giant

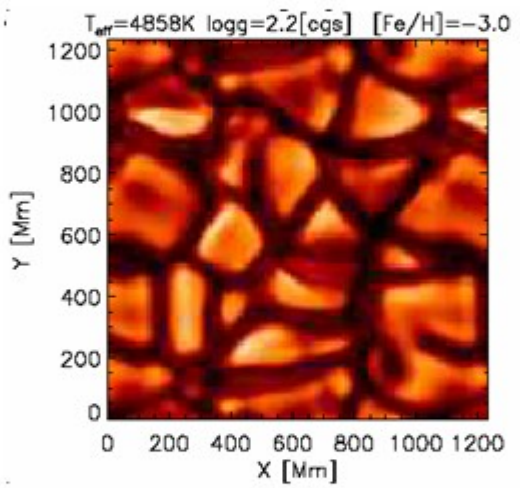

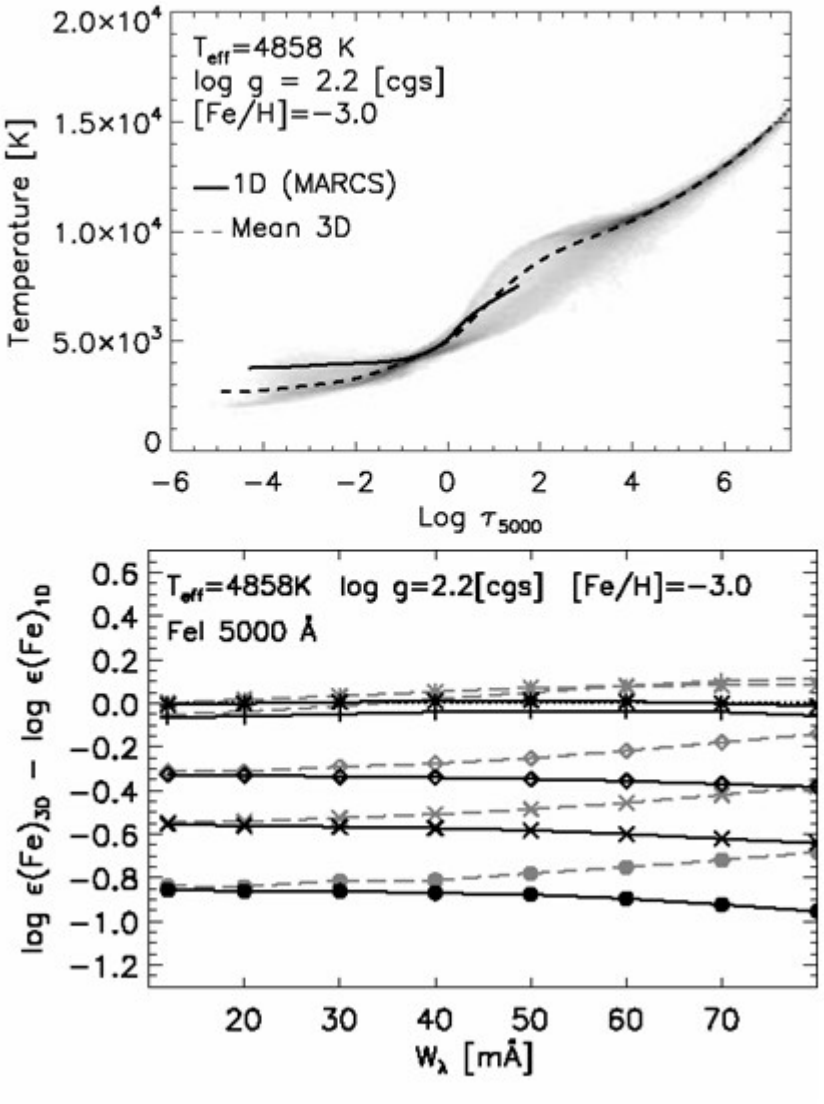

→ Extremely large 3D (LTE) corrections (~1dex!)

→ Need more physics (NLTE, scattering, OS)

Collet et al. (2007)

Solar limb darkening

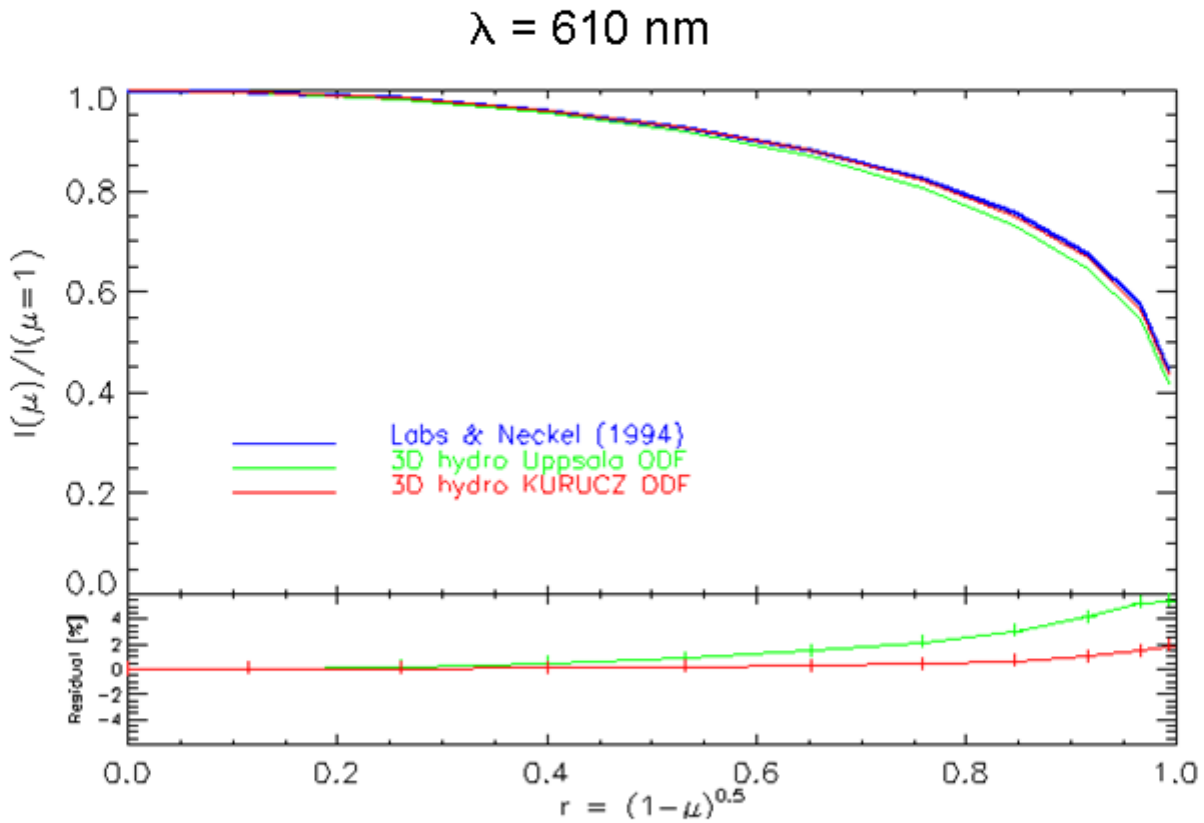

Very good fit in the visible → application to the **Picard** space Mission

- **Super granulation simulations** 48 × 20 Mm (Stein, Benson, Nordlund, 2006)

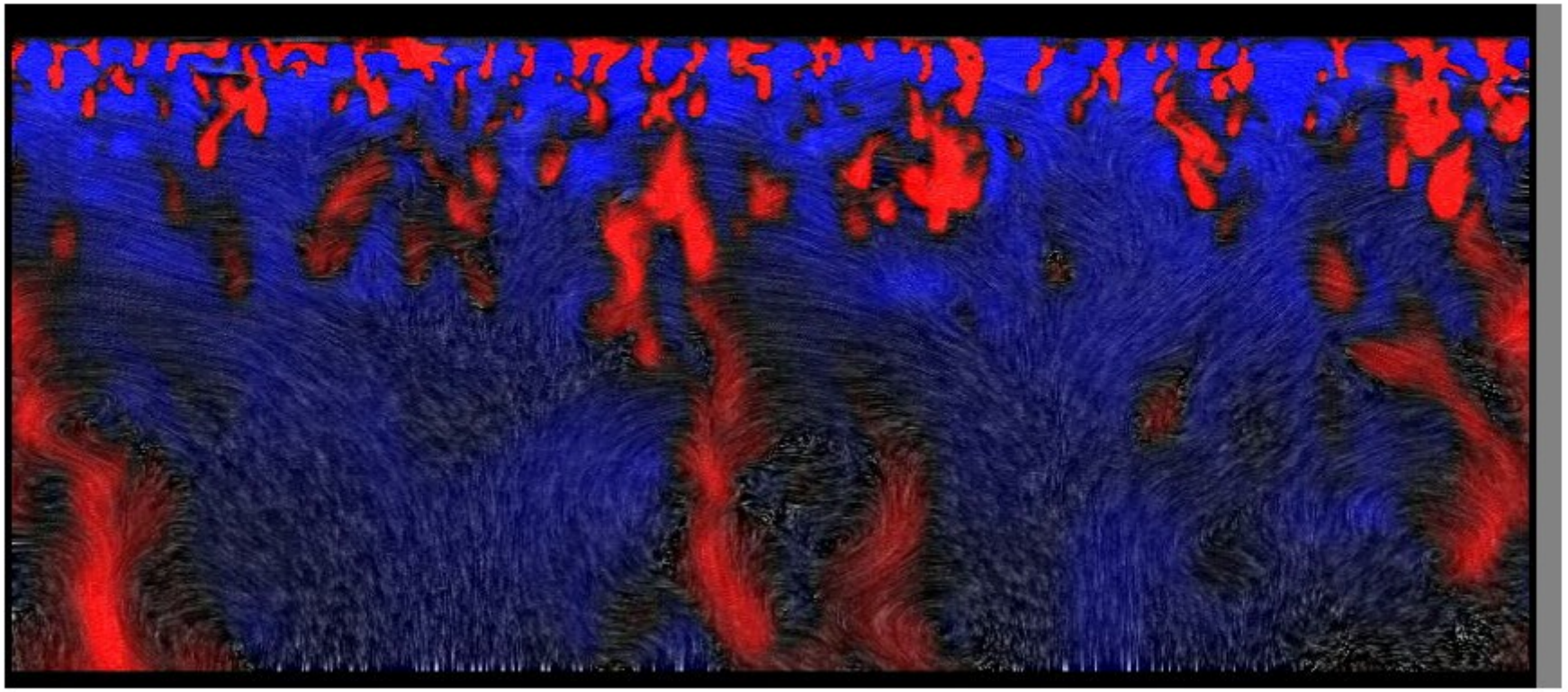

Courtesy Chris Henze

■ Magnetic field effects

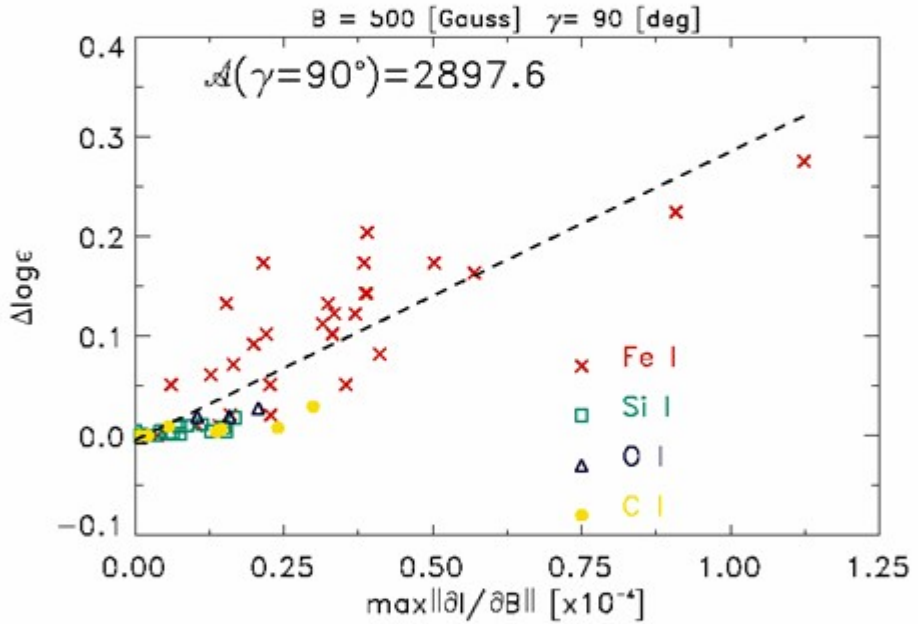

Borrero (2007, astro-ph, arXiv:0709.3809)

→ mostly affect FeI lines (~ 0.1dex)

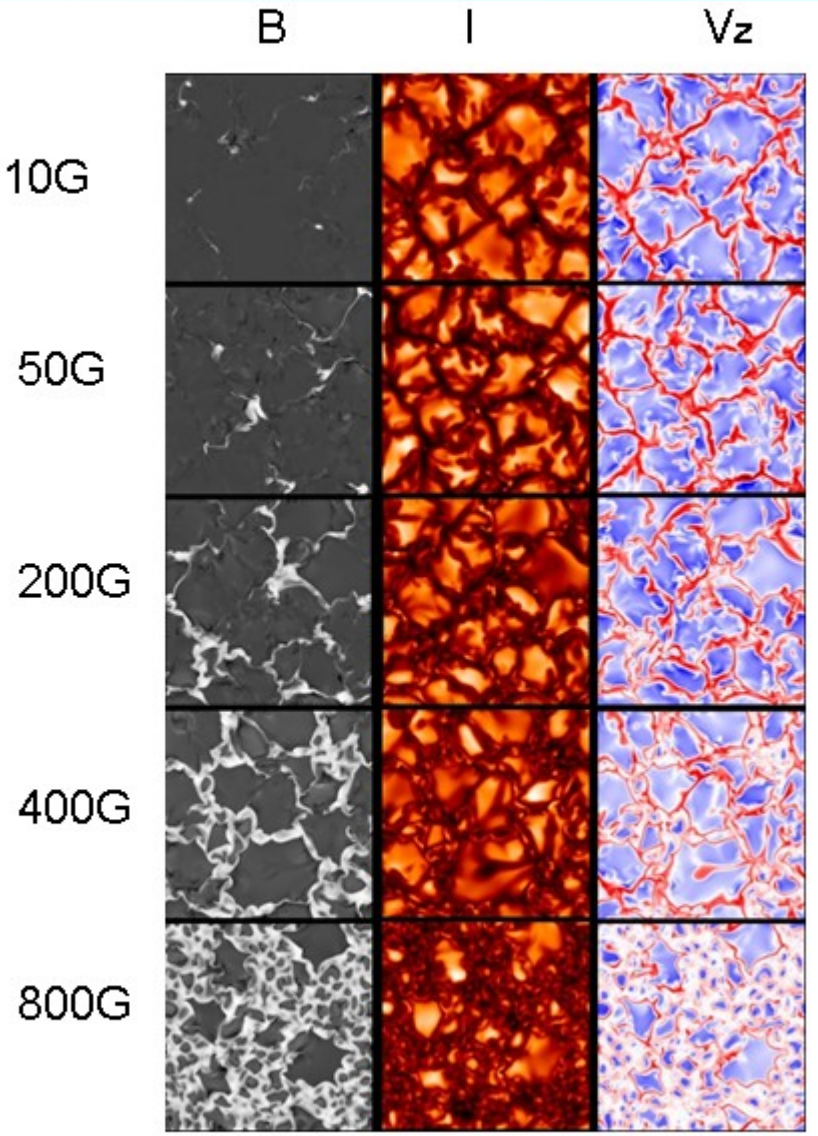

Courtesy A. Vögler, M. Schüssler

Summary

Surface convection simulations

Realistic modelling of stellar photospheres
Applicable to many types of stars: solar, metal-poor/rich, Red giant, M-dwarf
No longer need of micro and macro turbulence.

Solar simulations were successful to reproduce:

Granulation topology
Intensity brightness rms
Limb-darkening
Spectral lines (asymmetries, shifts)

(However, the new CNO abundances disagree with helioseismology …)

Perspectives

- More systematic use of 3D NLTE line transfer, need of atomic data (Léopoldine Brand Ph.D.)
- Toward full 3D NLTE convection simulations (for e.g. Red Giant)
- Role of magnetic fields for stellar abundances

Applications :

Local helioseismology
Limb darkenings → Interferometry (**VLTI**/AMBER+VINCI), **Picard**
Abundance determination, radial velocities → **Gaia**
Asteroseismology → **Corot**